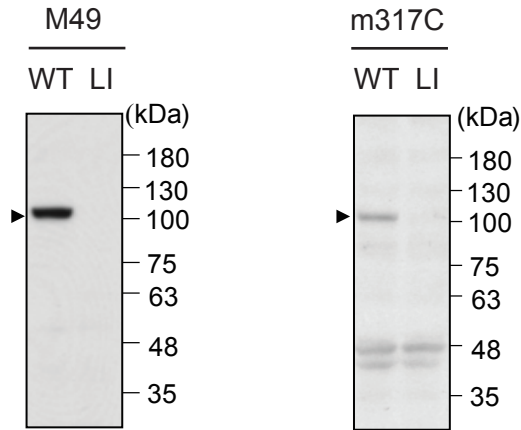


Supplementary Fig. 1. PDE4 activity was augmented in a cell model of Htt with expanded polyglutamine (polyQ).

PDE4 activity of neuro2a cells overexpressing Htt67Q150-EGFP (Q150) was higher than that of the cells overexpressing Htt67Q16-EGFP (Q16) at 5 days after the expression of Htt-EGFP. Data represent mean + SEM (4 independent sample sets). ** $P < 0.01$; Unpaired two tailed t-test.

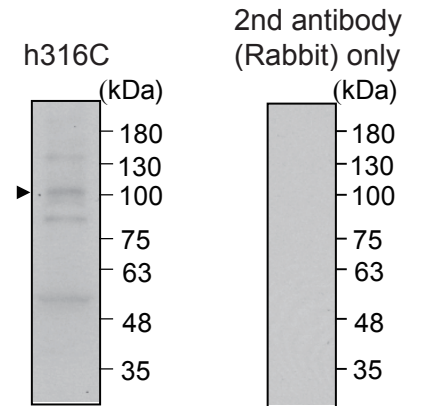
A

Western blotting
mouse DISC1 antibody



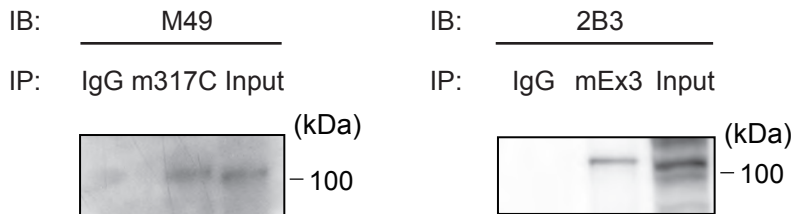
B

Western blotting
human DISC1 antibody



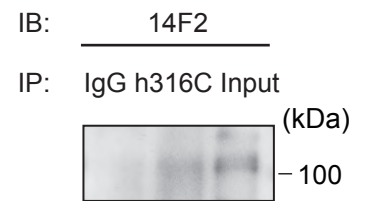
C

IP-Western
mouse DISC1 antibody



D

IP-Western
human DISC1 antibody

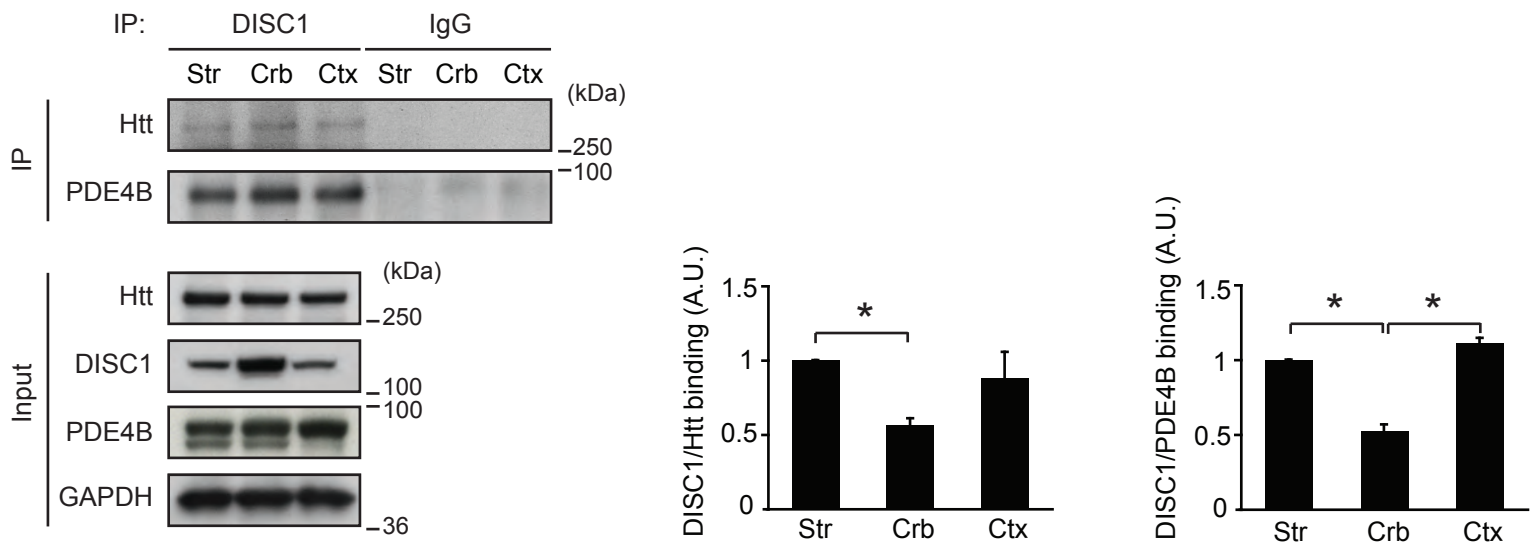


Supplementary Fig. 2. Validation of mouse or human DISC1 antibodies used in this study.

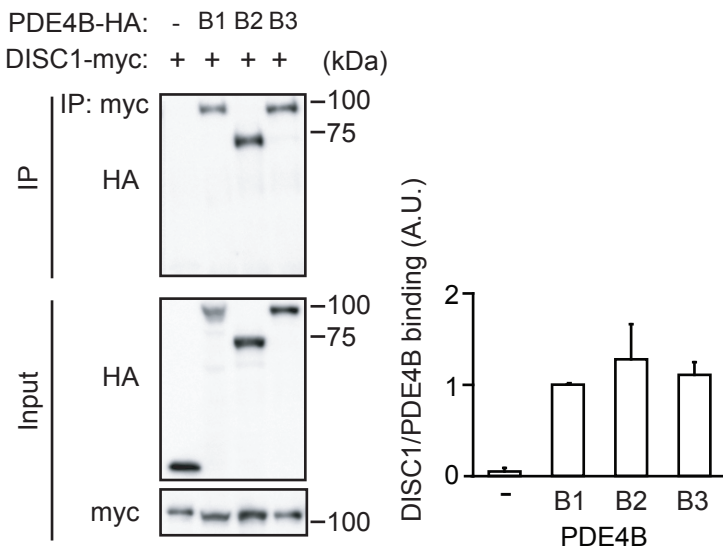
(A) Monoclonal or polyclonal anti-mouse DISC1 antibodies were validated by western blotting in wild-type (WT) and Disc1 Locus Impairment (LI) mouse cerebral cortex (Shahani et al., 2015; Seshadri et al., 2015). (B) A rabbit polyclonal anti-human DISC1 antibody was used for western blotting in human cerebral cortex. (C) Left: Co-immunoprecipitation with mouse brains by a mouse DISC1 m317C antibody, followed by immunoblotting with a mouse DISC1 M49 antibody. Right: Co-immunoprecipitation with mouse brains by a mouse DISC1 mEx3 antibody (Ishizuka et al., 2007; Shahani et al., 2015; Seshadri et al., 2015), followed by immunoblotting with a mouse DISC1 2B3 antibody (Shahani et al., 2015). (D) Co-immunoprecipitation with human brains by a human DISC1 h316C antibody, followed by immunoblotting with a human DISC1 14F2 antibody (Ottis et al., 2011). Arrowheads indicate full length DISC1.

Representative immunoblots are shown from 2-3 independent sample sets.

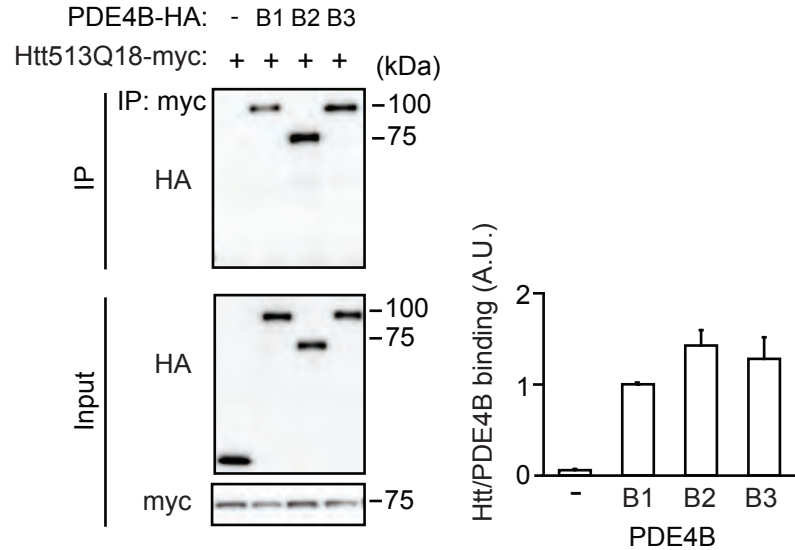
A



B



C



Supplementary Fig. 3. DISC1 binding to Htt and PDE4B was observed in distinct brain regions, and both DISC1 and Htt bind to PDE4B isoforms.

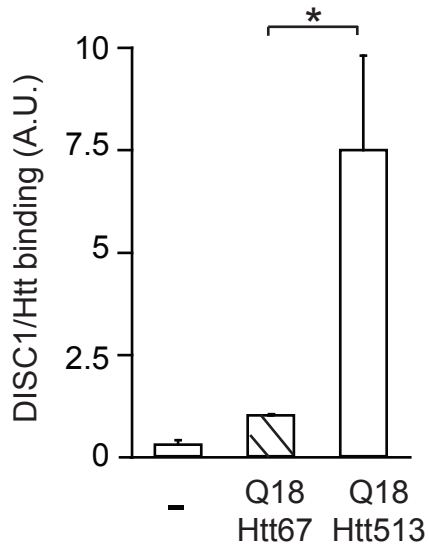
(A) Immunoprecipitation with an anti-DISC1 antibody (m317C) showed that the binding of DISC1 (M49) to Htt (MAB2166) and PDE4B (pan PDE4B) was observed in distinct brain regions such as striatum, cerebral cortex and cerebellum. Each interaction was more significant in striatum and cerebral cortex than cerebellum. * $P < 0.05$.

(B) Binding of DISC1 to PDE4B isoforms in HEK293T cells by co-immunoprecipitation.

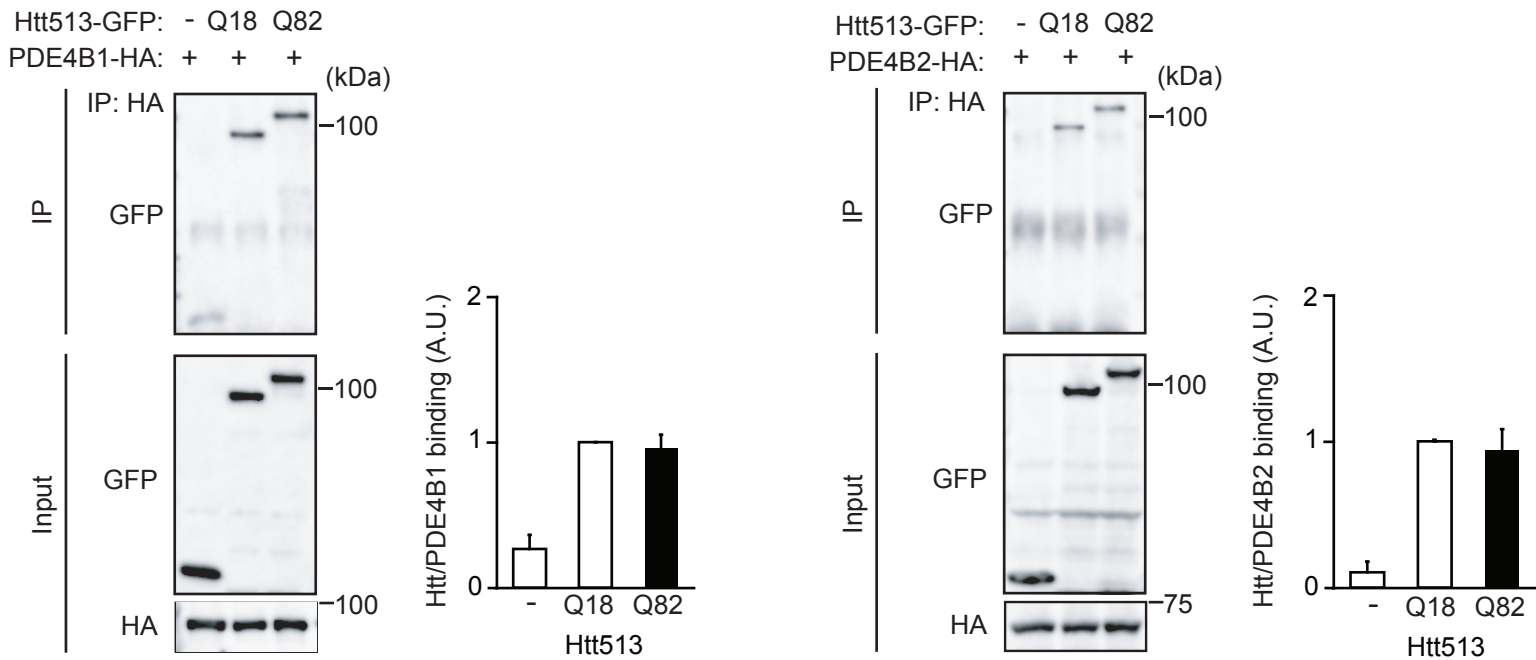
(C) Binding of Htt to PDE4B isoforms in HEK293T cells by co-immunoprecipitation.

Data represent mean + SEM (3 independent sample sets). P -values were determined by one-way ANOVA followed by Bonferroni post-hoc corrections.

A



B



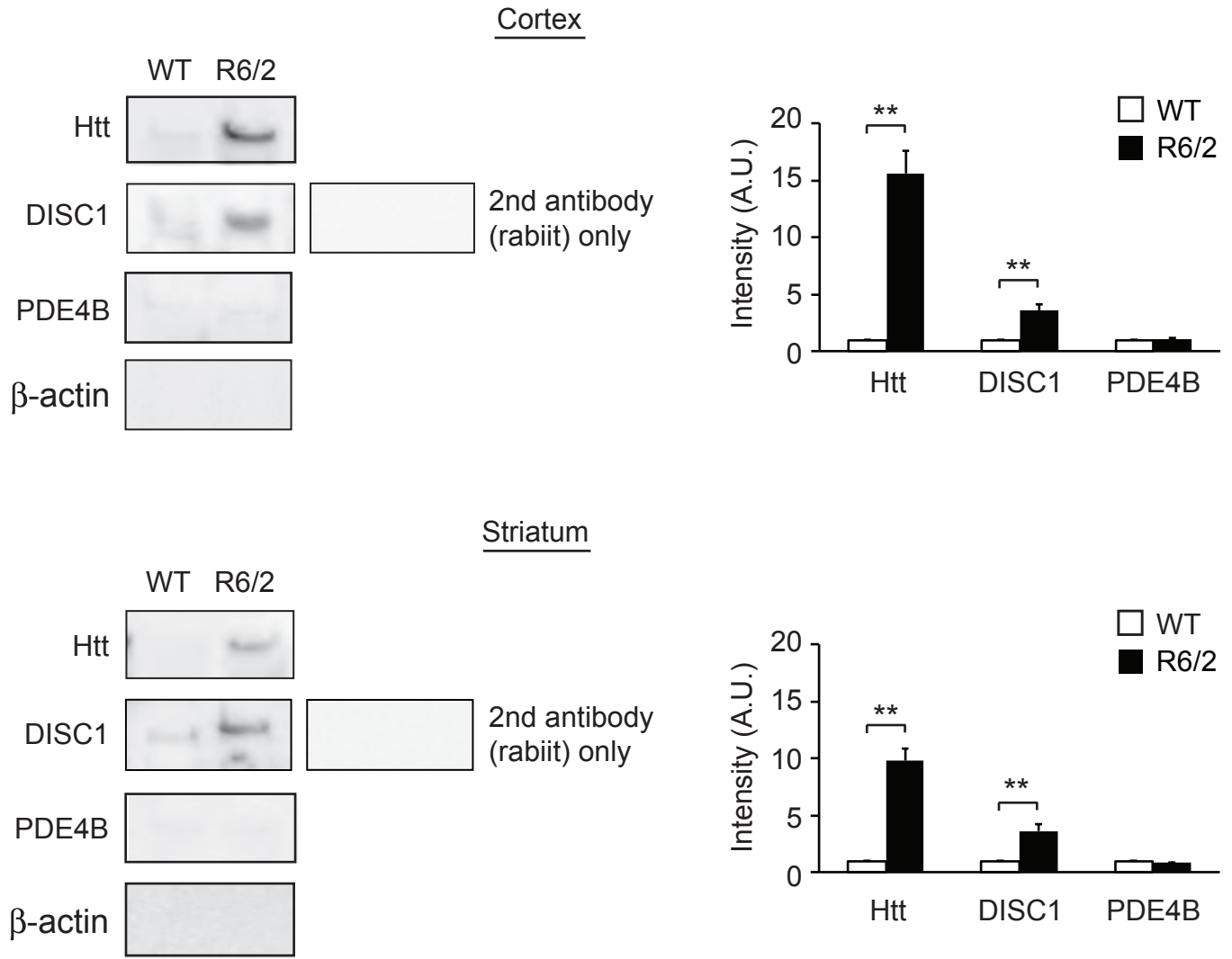
Supplementary Fig. 4. DISC1 binding to Htt513 was increased, compared to that to Htt67, and polyQ expansion in Htt had no effects on its binding to PDE4B isoforms.

(A) Increased binding of DISC1 with Htt513, compared to that with Htt67, in HEK293T cells by co-immunoprecipitation. * $P < 0.05$.

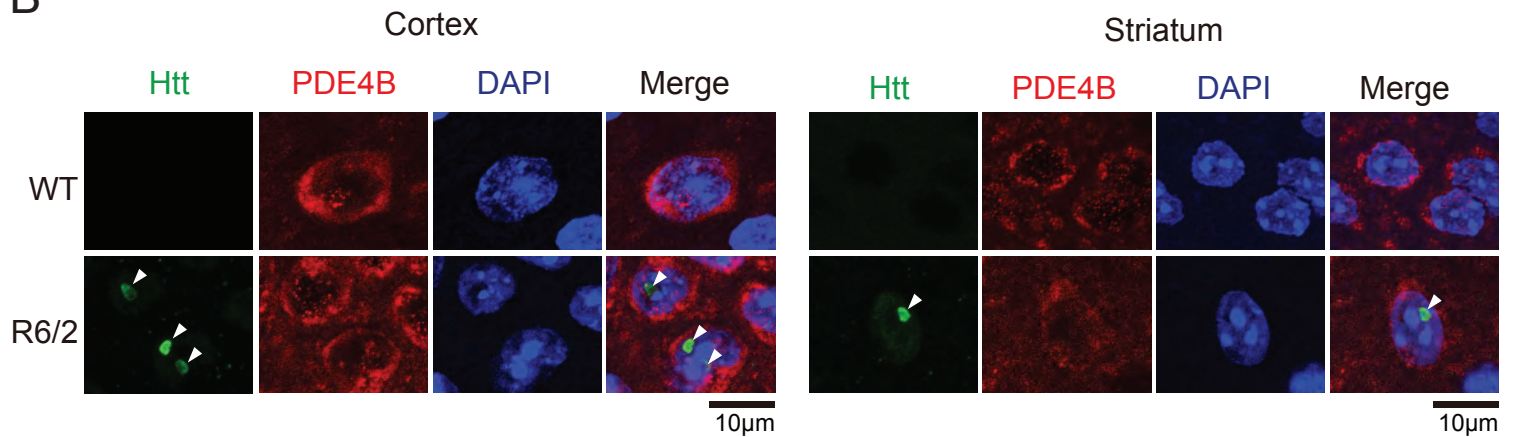
(B) No change in binding of Htt513 with PDE4B isoforms by polyQ expansion in Htt in HEK293T cells by co-immunoprecipitation.

Data represent mean + SEM (3 independent sample sets). P -values were determined by one-way ANOVA followed by Bonferroni post-hoc corrections.

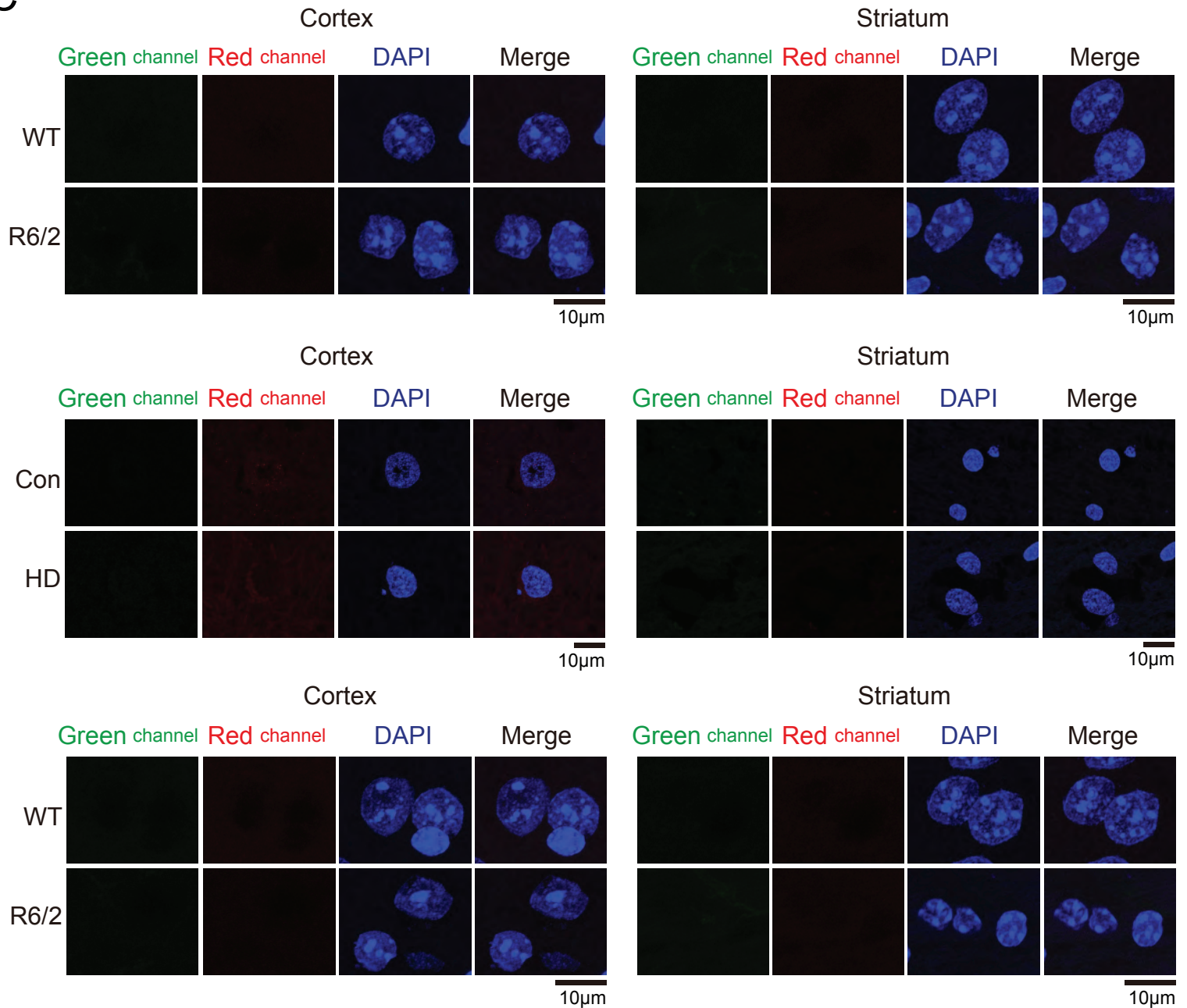
A



B



C



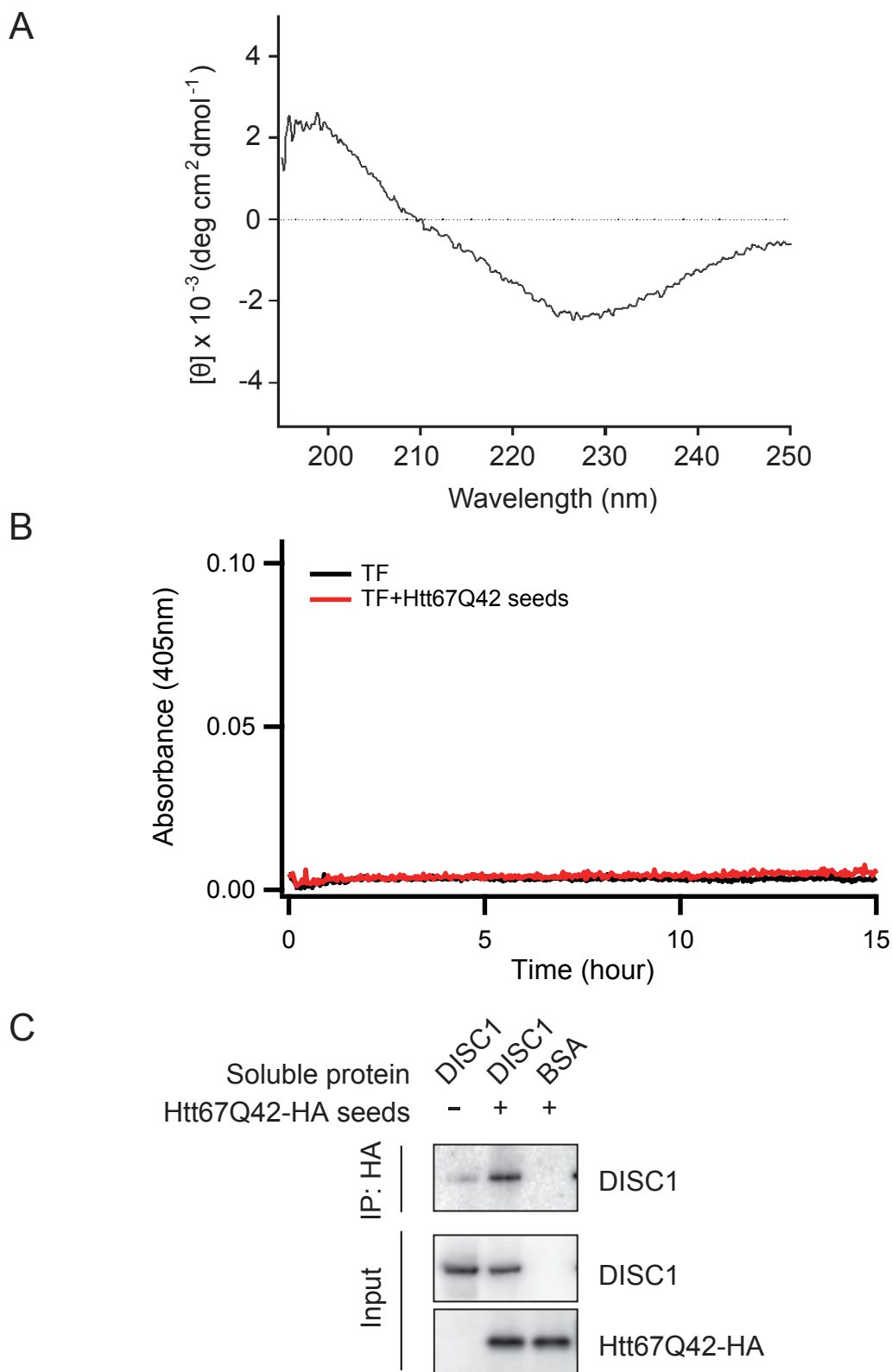
Supplementary Fig. 5. SDS-resistant aggregates of DISC1 and no colocalization of PDE4B with intranuclear inclusions of Htt were observed in R6/2 mice.

(A) Immunoreactivities of DISC1 (m317C) and Htt (EM48), but not that of PDE4B (pan PDE4B), in total homogenates (in 2% SDS) from cerebral cortex (upper) or striatum (lower) in R6/2 mice were observed on the top of the gel. No immunoreactivity of DISC1, Htt, or PDE4B was detected in wild-type (WT) mice. β -actin is a loading control. Data represent mean + SEM. $**P < 0.01$; Unpaired two tailed t-test. $n = 3$ per group.

A negative control with rabbit secondary antibody alone was also shown.

(B) Immunostaining of frozen sections of cerebral cortex (left) or striatum (right) demonstrated that PDE4B was not colocalized with intranuclear inclusions of mutant Htt in 12-week-old R6/2 mice. Green, Htt (EM48); PDE4B (pan PDE4B); blue, DAPI (the nucleus). Arrowheads show intranuclear inclusions. Scale bar, 10 μ m. $n = 3$ per group

(C) Negative controls for immunohistochemistry with no primary antibodies: upper, corresponding to Figure 2C ($n = 3$ per group); middle, corresponding to Figure 2D [$n = 3$ (Con), 6 (HD)]; bottom, corresponding to Supplementary Figure 5B ($n = 3$ per group).



Supplementary Fig. 6. Characterization of in vitro DISC1 aggregates

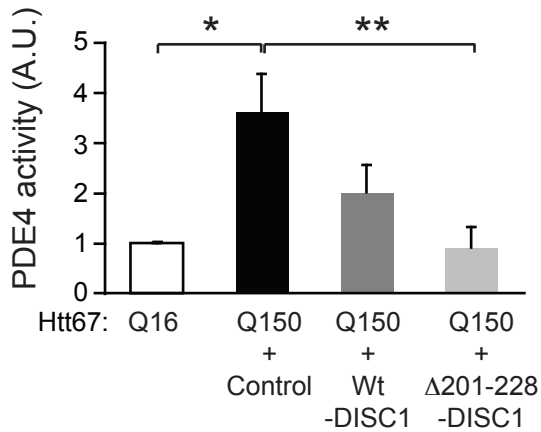
(A) A Far-UV CD spectrum of DISC1 aggregates showed a negative peak at 228 nm, indicating the presence of β -sheet-rich structures. Representative data is shown from 2 independent samples.

(B) Aggregation of trigger factor (TF) in the absence or presence of Htt67Q42 aggregate seeds was monitored by the absorbance (turbidity) at 405 nm. No acceleration of TF aggregation was observed. Representative data is shown from 2 independent sample sets.

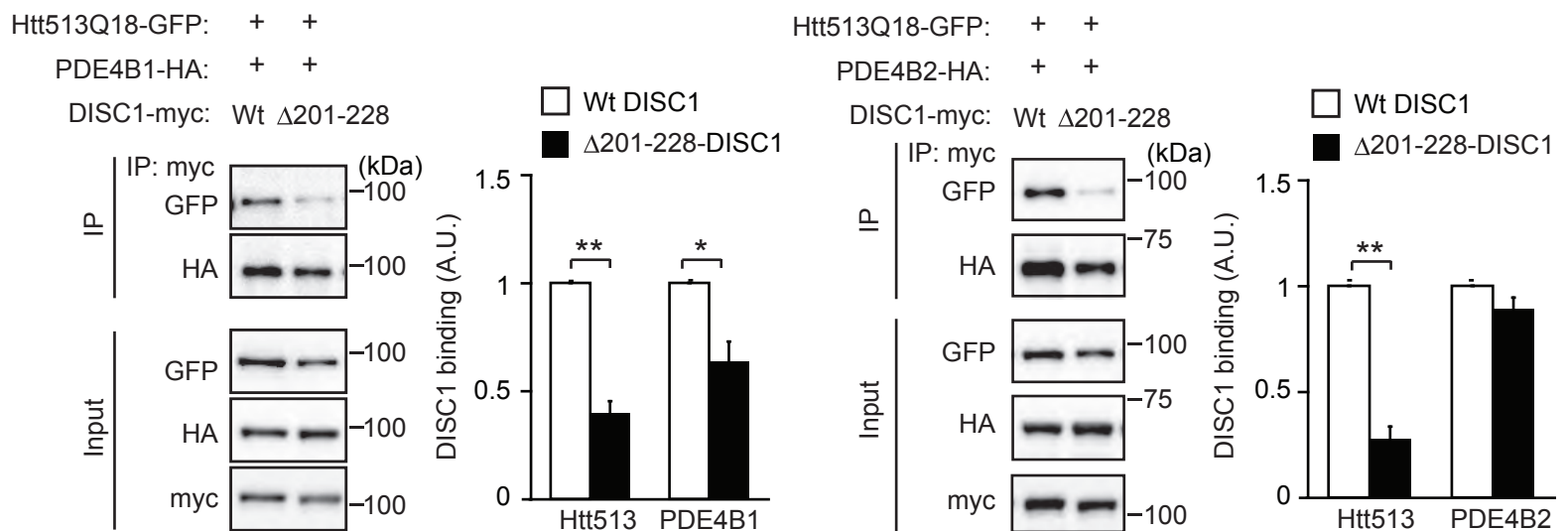
(C) Co-aggregation of Htt67Q42 seeds and DISC1 monomer.

DISC1 or BSA monomer was incubated in the presence or absence of HttQ42-HA seeds (10% mol/mol). The resulting aggregates were immunoprecipitated with anti-HA beads and immunoblotted by an anti-DISC1 h316C polyclonal antibody. Representative immunoblots are shown from 3 independent sample sets.

A



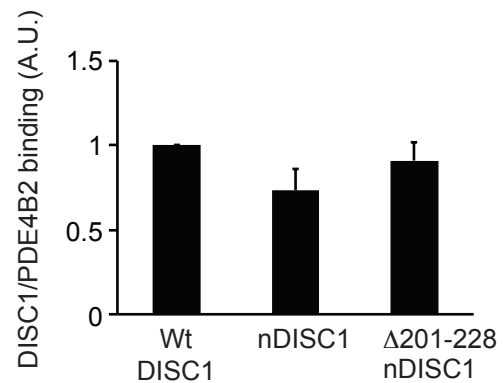
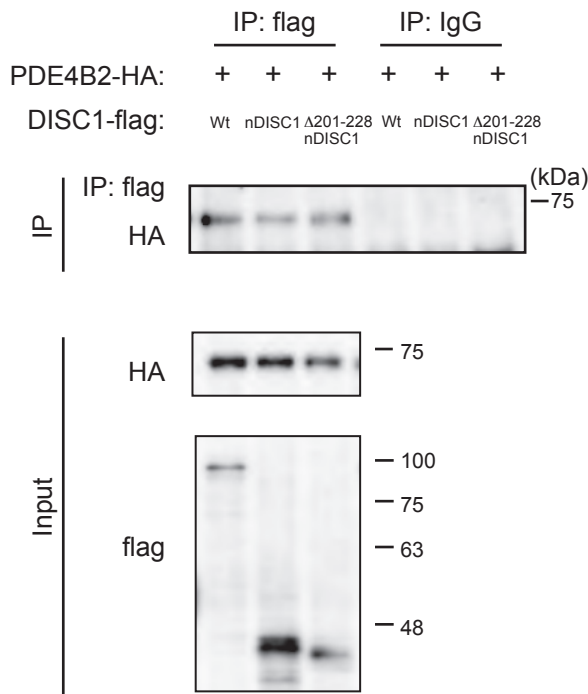
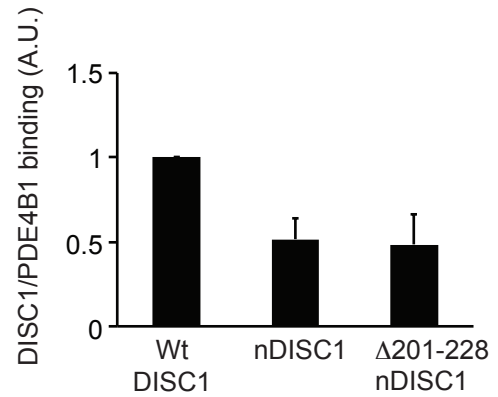
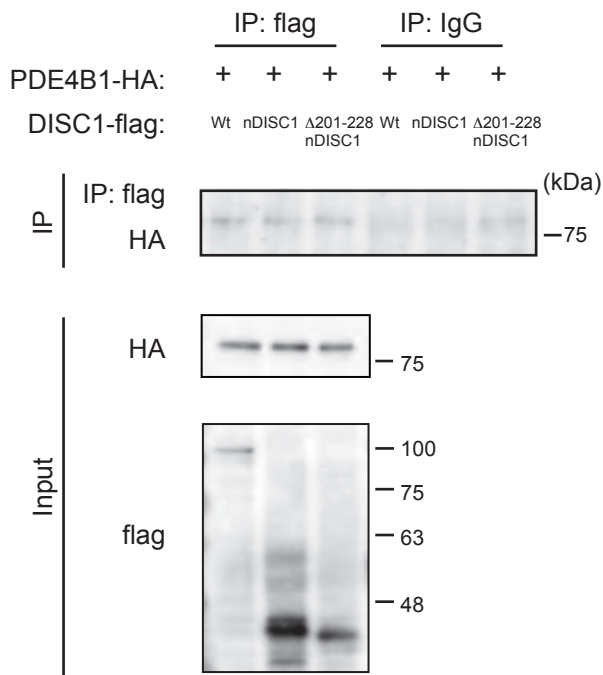
B



Supplementary Fig. 7. Aberrantly enhanced PDE4 activity was normalized by exogenous DISC1 expression, and deletion mutant DISC1 lacking residues 201-228 showed significantly reduced binding with Htt513Q18 but maintained interactions with PDE4B.

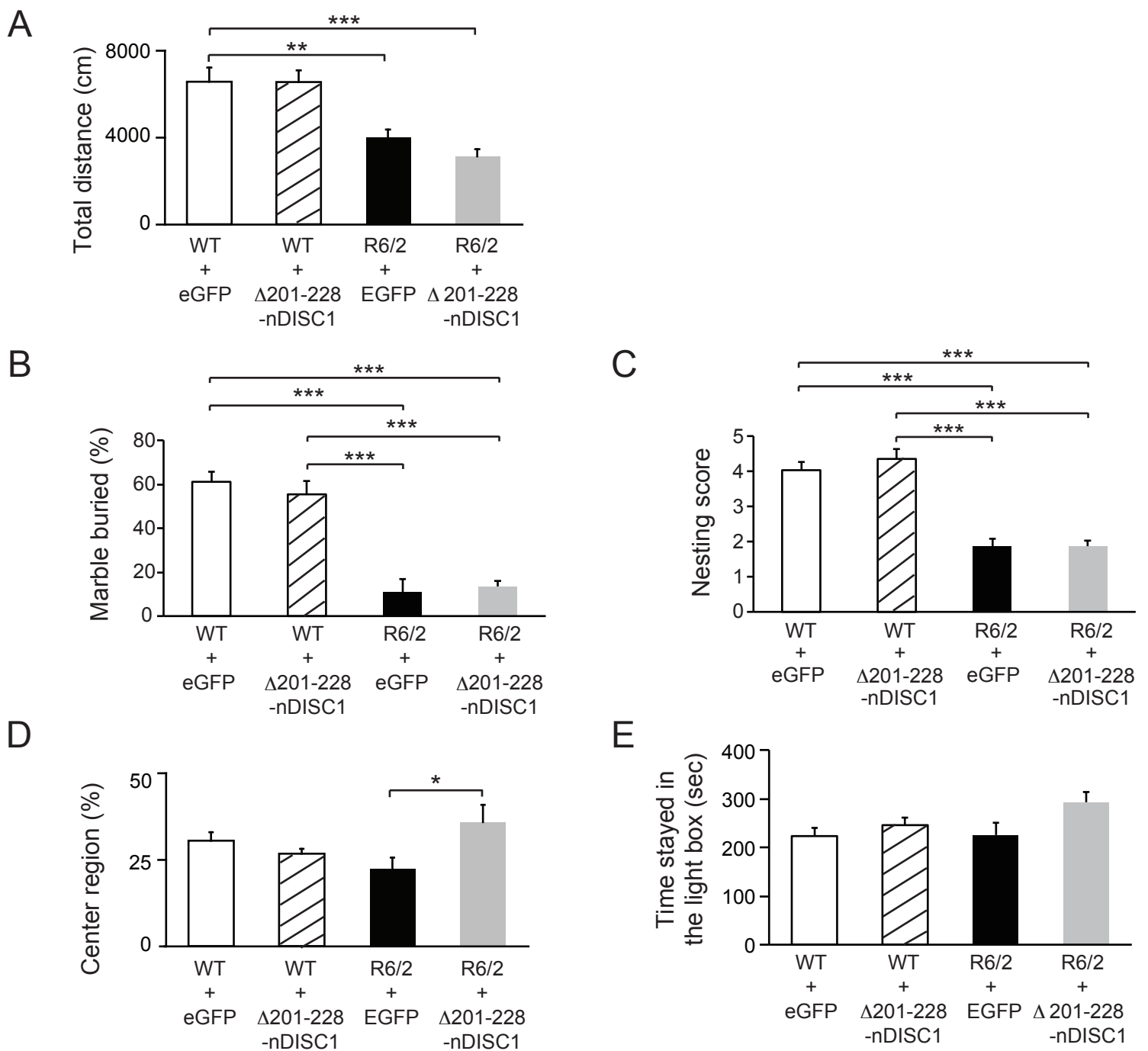
(A) Aberrant augmentation of PDE4 activity in neuro2a cells at 5 days after the induction of Htt67Q150-EGFP was ameliorated with a transient co-expression of wild-type (Wt) or deletion mutant DISC1 lacking the binding site for Htt (Δ 201-228-DISC1). Data represent mean + SEM (5 independent sample sets). * P <0.05, ** P <0.01; One-way ANOVA followed by Bonferroni post-hoc corrections.

(B) Deletion mutant DISC1 lacking residues 201-228 showed a decrease in binding with Htt513Q18, but still maintained interactions with PDE4B isoforms, PDE4B1 (left) and PDE4B2 (right), in HEK293T cells. Data represent mean + SEM (3 independent sample sets). * P <0.05, ** P <0.01; Unpaired two tailed t-test.



Supplementary Fig. 8. N-terminal domain (amino acid residues 1-316) of mouse DISC1 lacking the binding region for Htt (Δ 201-228-nDISC1) maintained interactions with PDE4B.

Co-immunoprecipitation experiments showed that Δ 201-228-nDISC1 maintained interactions with PDE4B isoforms, PDE4B1 (upper) and PDE4B2 (lower), in HEK293T cells. Data represent mean + SEM (3 independent sample sets). Statistical analyses were conducted by one-way ANOVA.



Supplementary Fig. 9. Open field, light/dark transition, marble burying, and nesting behavioral phenotypes

(A) The locomotor activity of R6/2 mice was not affected by expression of $\Delta 201-228$ -nDISC1. Total distance moved in the open field test was measured in mice at 8 weeks. $n=15, 15, 18, 17$ for WT+EGFP, WT+ $\Delta 201-228$ -nDISC1, R6/2+EGFP, R6/2+ $\Delta 201-228$ -nDISC1 mice, respectively. $**P<0.01$, $***P<0.001$.

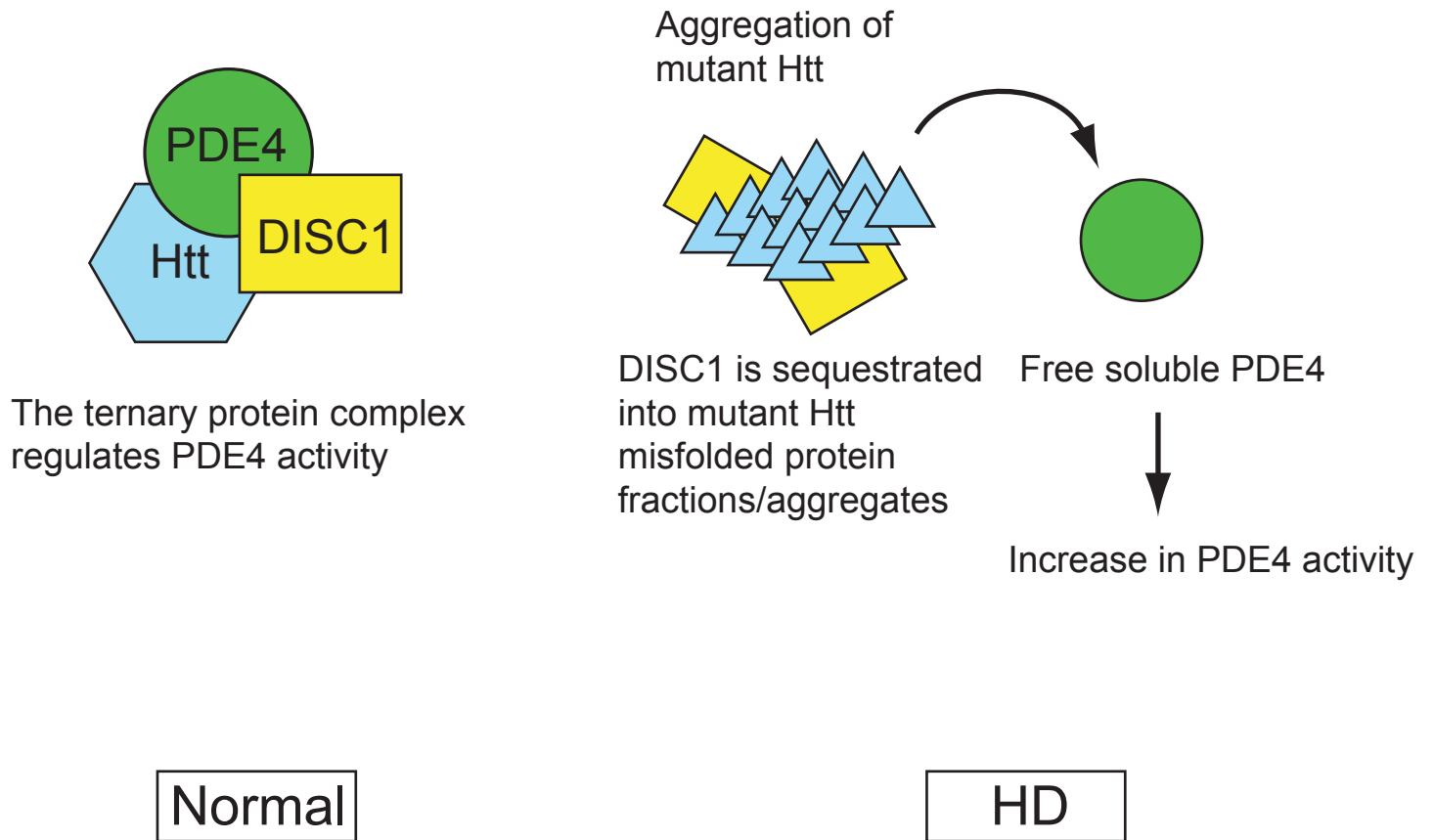
(B) Marble burying defects in R6/2 mice were not rescued by $\Delta 201-228$ -nDISC1 expression. The marble burying test was performed in mice at 8 weeks. $n=15, 16, 16, 22$ for WT+EGFP, WT+ $\Delta 201-228$ -nDISC1, R6/2+EGFP, R6/2+ $\Delta 201-228$ -nDISC1 mice, respectively. $***P<0.001$.

(C) Deficits of nest building behaviors in R6/2 mice were not rescued by $\Delta 201-228$ -nDISC1 expression. The nesting behavior was examined in mice at 8 weeks. $n=19, 17, 18, 18$ for WT+EGFP, WT+ $\Delta 201-228$ -nDISC1, R6/2+EGFP, R6/2+ $\Delta 201-228$ -nDISC1 mice, respectively. $***P<0.001$.

(D) The anxiety levels in R6/2 mice were reduced by expression of $\Delta 201-228$ -nDISC1. The time spent in a center region in the open field test was measured in mice at 8 weeks. $n=15, 15, 18, 17$ for WT+EGFP, WT+ $\Delta 201-228$ -nDISC1, R6/2+EGFP, R6/2+ $\Delta 201-228$ -nDISC1 mice, respectively. $*P<0.05$.

(E) The anxiety levels in R6/2 mice were examined by the dark/light transition test. The time spent in the light box was measured in mice at 8 weeks. $n=18, 24, 19, 25$ for WT+EGFP, WT+ $\Delta 201-228$ -nDISC1, R6/2+EGFP, R6/2+ $\Delta 201-228$ -nDISC1 mice, respectively.

Data represent mean + SEM. P -values were determined by one-way ANOVA followed by Bonferroni post-hoc corrections.



Supplementary Fig. 10. Model for the ternary protein complex consisting of Htt, DISC1 and PDE4.

The ternary protein complex of Htt, DISC1 and PDE4 is impaired by co-aggregation of DISC1 into polyQ-expanded mutant Htt misfolded protein fractions/aggregates, releasing functional PDE4, which increases PDE4 activity and possibly affects non-motor functions.